Ergodic Capacity Performance of D2D IoT Relay NOMA-SWIPT Systems with Direct Links

Ashish Rauniyar[†*], Paal Engelstad[†*], Olav N. Østerbø[‡]
[†]Department of Technology Systems, University of Oslo, Norway
[*]Department of Computer Science, OsloMet - Oslo Metropolitan University, Norway
[‡]Telenor Research, Norway
Email: (ashish.rauniyar, paal.engelstad)@oslomet.no, olav.osterbo@getmail.no

***Abstract*—We investigate the Ergodic capacity (EC) performance of device-to-device (D2D) Internet of Things (IoT) relay non-orthogonal multiple access (NOMA)- simultaneous wireless information and power transfer (SWIPT) systems where the relayed communication is supported with direct link. A two-user case is considered in which a base station transmits symbols to two NOMA users, and the energy harvesting (EH) based relay node via a direct link. The EH based relay node harvests the energy from the BS's signal and again transmits a superimposed composite NOMA signal intended for the user with poor channel condition and for its D2D user to offload its data traffic. A D2D user offloading is considered to further enhance the spectral efficiency of the system. We derive the analytical expressions for the EC of each of the user and the ergodic sum capacity (ESC) of the system and validate them with simulation results. In such settings, our results demonstrate that the EC of a node and the ESC of the system can be improved through the maximal ratio combining (MRC) scheme compared to a system with single signal decoding scheme. Our results also indicate that the overall ESC of the NOMA-SWIPT system can be improved by having a direct link for a user in the system.**

***Keywords*—Internet of Things, Energy Harvesting, NOMA, Direct link, D2D, SWIPT, Ergodic capacity.**

I. Introduction

The Internet of Things (IoT) is about to become an integral part of our daily life with various applications targeting the smart home, smart city, smart health, smart transportation, automation, and so on [1]. Since, IoT and its applications are integrating into our daily life, the number of IoT devices are expected to skyrocket at an unprecedented rate. Reference [2] has already predicted that 125 billion IoT devices will be connected to the Internet by 2030. IoT is considered as one of the important parts of the fifth-generation (5G) networks [3]. The 5G and the next generation networks are expected to be spectrally efficient to support the massive connectivity requirements of IoT [4]. Moreover, usually, these IoT devices are battery-operated [5]. Replacing or charging the battery of IoT devices or networks is often not a feasible option, especially if it is deployed in chemical plants, nuclear reactors, underground tunnels, and so on. Thus, energy-efficient data transmission of IoT devices is a major concern [6]. In this regard, non-orthogonal multiple access (NOMA) and simultaneous wireless information and power transfer (SWIPT) have been contemplated as a key technology for enhancing spectral and energy-efficiency to support IoT devices requirements in the next generation of wireless networks [7].

In NOMA, multiple user's signals can be transmitted at the same time using the same frequency, and code. Specifically, in power domain NOMA, multiple user signals are multiplexed in a power domain so that the users with poor channel conditions are allocated more power compared to the users with better channel conditions [8]. In NOMA, the transmitter uses a superposition coding scheme to multiplex different user signals, and the receiver uses a signal-to-interference cancellation (SIC) technique to decode and cancel the signal of the users with poor channel conditions before decoding its own signal [9].

Relaying nodes represents a practical solution for extending the life-time and coverage of the network [10]. These relay nodes of a network can be self-powered through SWIPT [11]. Thus eliminating the need for extra power supply within the network. However, SWIPT cannot be applied directly for the information decoding due to the practical consideration of the energy harvesting (EH) receivers. Therefore, time-switching and power splitting relaying are two popular EH architectures widely considered for SWIPT [12]. In this paper, we focus on the power splitting architecture because it often performs better than the TS architecture [13].

A radio frequency (RF) EH and information transmission system based on NOMA for the wireless powered system was studied in [14]. Here, the authors thoroughly investigated the performance of PS architecture for a system model in which an EH based relay node assisted the source node to transmit its data, and at the same time it also transmitted or offloaded its data traffic to its destination node using the NOMA protocol. Further, the authors in [15] extended the model by introducing the interfering signal in the system and investigated its performance. However, no direct links were considered in their system model, and the data transmission was done only through the relay link. In severe fading or shadowing cases, it is reasonable to assume that no direct link exists between the source and the destination node. However, in moderate fading or shadowing environments, usually direct links exist. Consolidating these direct links in the system could significantly enhance the performance of the cooperative relaying systems [16]. A joint relay-user selection in an EH relay network with a direct link was investigated in [17]. Here, the authors investigated the outage probability of the amplify-

DOI: https://doi.org/10.1109/TSP49548.2020.9163552

and-forward full-duplex (FD) relay network, which included one source node, a multi-relay node, and a multi-user node. The direct link between the source node and the user node was considered to convey information.

The authors in [18] investigated the outage performance of dual-hop decode-and-forward (DF) relay systems in the presence of a direct link between the source and the destination node where SWIPT was exploited at the relay by using a static/dynamic PS scheme. In [19], the outage performance of EH DF relaying NOMA networks with direct links was studied. However, the authors did not analyze the ergodic capacity (EC) of the system model in the presence of direct links. Studying and analyzing the EC and the ergodic sum capacity (ESC) of a system is important, especially for delay-tolerant transmissions where the source can transmit at any rate upper bounded by the EC. Therefore, motivated by these works, in this paper, we investigate the EC performance of NOMA-SWIPT aided D2D IoT relay systems with direct links. We consider a two-user case where a base station (BS) transmits symbols to two NOMA users and to the EH based relay node via a direct link. The PS EH based relay node harvests the energy from the BS's signal and again transmits a superimposed composite NOMA signal intended for the user with poor channel condition and for its device-to-device (D2D) user. The reason we have considered a D2D user in the considered system is to assist the EH based relay node for offloading its data traffic and thereby further enhancing the spectral efficiency of the considered system.

In summary, the major contributions of this paper are as follows:

- Unlike existing works, our proposed system model is more practical as we have assumed that the UE_2 user has a strong direct link with the BS, and the UE_1 user has a weak direct link from the BS. Therefore, the data of UE_1 has to be re-transmitted again via an EH based relay node UE_3. Further, UE_3 not only forwards the data of UE_1, but it will also transmit the data for its D2D user, i.e. UE_4 to offload its data traffic.
- To show the impact of direct links, we have used the single signal decoding (SDS), and the maximal ratio combining (MRC) scheme and derive its analytical expressions for the EC and ESC. We show the performance gains in terms of ESC of the system by using MRC scheme.
- Effect of transmit SNR and other EH parameters on the EC and ESC performance for both the MRC and SDS schemes were investigated to gain further insight into the NOMA-SWIPT system.

II. System Model

The considered cooperative NOMA-SWIPT aided D2D IoT relay system model with direct links is shown in Fig. 1. Here, a BS will transmits two symbols, x_1 and x_2 to UE_1 and UE_2, respectively, through the direct links. UE_1 is considered as a distant user with poor channel conditions compared to UE_2. As UE_3 is a power constrained node that acts as a DF relay,

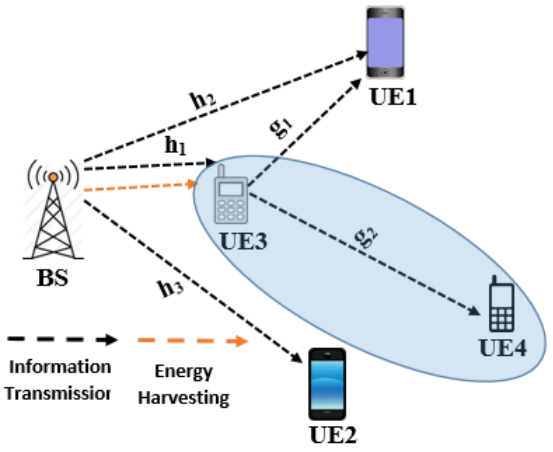

Fig. 1. Considered system model for NOMA-SWIPT with direct link

it first harvests the RF energy from the signal of BS using the PS protocol and then decodes the symbols x_1 and x_2 transmitted by the BS in the first phase. Also UE_1 and UE_2 receives the information transmitted by the BS through the direct link in the first phase. Since UE_1 is a distant user with poor channel conditions compared to UE_2, the symbol x_1 is re-transmitted via a energy constrained relay node UE_3. Further to improve the spectral efficiency of the considered NOMA-SWIPT system, we have considered that UE_3 will also transmit or offload its data traffic to its D2D user UE_4 to enhance the spectral efficiency of the system. Thus, UE_3 forwards the symbol x_1 and x_r using the NOMA protocol to UE_1 and UE_4 in the subsequent phase.

We have assumed that all nodes are operating in a half duplex mode. The channel state information (CSI) is assumed to be known at all nodes. Each of the communication channel faces an independent Rayleigh flat fading with additive white Gaussian noise (AWGN) with zero mean and variance σ^2. The complex channel coefficient between any two nodes is denoted by $h_i \sim CN(0, \lambda_{h_i} = d_i^{-v})$ and $g_j \sim CN(0, \lambda_{j_i} = d_j^{-v})$ where $i \in \{1, 2, 3\}$, $j \in \{1, 2\}$, $CN(0, \lambda_{h_i} = d_i^{-v})$ and $CN(0, \lambda_{g_j} = d_j^{-v})$ are complex normal distributions to model the Rayleigh flat fading channel with zero mean variance λ_{h_i},λ_{g_j} and d_i, d_j are the distances between the two nodes on the corresponding link, and v is the path loss exponent. Without loss of generality, it is assumed that $|h_1|^2 > |h_3|^2 > |h_2|^2$ and $|g_1|^2 > |g_2|^2$. Therefore, $\lambda_{h_1} > \lambda_{h_3} > \lambda_{h_2}$ and $\lambda_{g_1} > \lambda_{g_2}$. Under the availability of statistical CSI, these assumptions represent an effective strategy that can be employed in the system, and it is in line with the previous works such as [20].

A. System Model based on PS Architecture

Here, a power-constrained node UE_3 splits the incoming signal into two parts: ϵP_s and $(1-\epsilon)P_s$ by a power splitting factor ϵ. UE_3 harvests energy from the signal of BS using ϵP_s, where P_s is the power of the BS transmit signal. UE_3

then uses the remaining power $(1-\epsilon)P_s$ for the information processing and decoding. The PS and NOMA in the considered system is working in two phases and these phases are explained in the following:

1) First Phase:

In the first phase, the BS broadcasts the following signal to UE_1, UE_2 and UE_3.

$$x = \sqrt{a_1 P_s}x_1 + \sqrt{a_2 P_s}x_2 \tag{1}$$

where a_1 and a_2 are NOMA power allocation coefficients and $a_1 > a_2$, $a_1 + a_2 = 1$.

The received signal at UE_3, UE_1 and UE_2 can be respectively given as:

$$y_{UE_3} = h_1(\sqrt{a_1 P_s}x_1 + \sqrt{a_2 P_s}x_2) + n_{UE_3} \tag{2}$$

$$y_{UE_1} = h_2(\sqrt{a_1 P_s}x_1 + \sqrt{a_2 P_s}x_2) + n_{UE_1} \tag{3}$$

$$y_{UE_2} = h_3(\sqrt{a_1 P_s}x_1 + \sqrt{a_2 P_s}x_2) + n_{UE_2} \tag{4}$$

where n_{UE_3}, n_{UE_1}, and $n_{UE_2} \sim CN(0, \sigma^2 = 1)$ denote the AWGN at UE_3, UE_1, and UE_2 respectively.

In the PS EH architecture, the EH and information decoding (ID) signal at UE_3 can be given as:

$$y_{UE_3,EH} = h_1(\sqrt{\epsilon a_1 P_s}x_1 + \sqrt{\epsilon a_2 P_s}x_2) + n_{UE_3} \tag{5}$$

$$y_{UE_3,ID} = h_1(\sqrt{(1-\epsilon)a_1 P_s}x_1 + \sqrt{(1-\epsilon)a_2 P_s}x_2) + n_{UE_3} \tag{6}$$

Now, the energy harvested at UE_3 can be given as:

$$P_{UE_3} = \eta\epsilon a_1 P_s|h_1|^2 + \eta\epsilon a_2 P_s|h_1|^2 = \eta\epsilon P_s|h_1|^2 = \eta\epsilon P_s X_1 \tag{7}$$

where $|h_1|^2 \sim X_1$ and η is the EH efficiency.

The signal-to-interference-noise ratio (SINR) for x_1 at UE_3, UE_1 and UE_2 can be respectively given as:

$$\gamma_{UE_3}^{x_1} = \frac{a_1(1-\epsilon)P_s|h_1|^2}{a_2(1-\epsilon)P_s|h_1|^2 + \sigma^2} = \frac{a_1(1-\epsilon)PX_1}{a_2(1-\epsilon)PX_1 + 1} \tag{8}$$

$$\gamma_{UE_1}^{x_1} = \frac{a_1 P_s|h_2|^2}{a_2 P_s|h_2|^2 + \sigma^2} = \frac{a_1 PX_2}{a_2 PX_2 + 1} \tag{9}$$

$$\gamma_{UE_2}^{x_1} = \frac{a_1 P_s|h_3|^2}{a_2 P_s|h_3|^2 + \sigma^2} = \frac{a_1 PX_3}{a_2 PX_3 + 1} \tag{10}$$

where $\frac{P_s}{\sigma^2} \sim P$ represents transmit SNR, $|h_2|^2 \sim X_2$ and $|h_3|^2 \sim X_3$.

Now, UE_3 and UE_2 decode the symbol x_2 by cancelling x_1 with SIC.

Therefore, the received SINR for x_2 at UE_3 and UE_2 can be respectively given as:

$$\gamma_{UE_3}^{x_2} = a_2(1-\epsilon)P|h_1|^2 = a_2(1-\epsilon)PX_1 \tag{11}$$

$$\gamma_{UE_2}^{x_2} = a_2 P|h_3|^2 = a_2 PX_3 \tag{12}$$

2) Second Phase:

To further improve the spectral efficiency as well as to offload its data traffic, UE_3 forwards the symbol x_1 and its own symbol x_r to UE_1 and UE_4 with transmit power P_{UE_3} by following the NOMA protocol. It is worth noting that since UE_1 is a distant user with poor channel conditions from the BS compared to UE_2, it is reasonable that the signal x_1 for UE_1 is retransmitted.

The received signal at UE_1 and UE_4 in the second phase can be respectively given as:

$$y_{UE_1}^{II} = g_1(\sqrt{b_1 P_{UE_3}}x_1 + \sqrt{b_2 P_{UE_3}}x_r) + n_{UE_1}^{II} \tag{13}$$

$$y_{UE_4}^{II} = g_2(\sqrt{b_1 P_{UE_3}}x_1 + \sqrt{b_2 P_{UE_3}}x_r) + n_{UE_4}^{II} \tag{14}$$

where b_1 and b_2 are NOMA power allocation coefficients and $b_2 > b_1$, $b_1 + b_2 = 1$.

Now, UE_4 decodes x_r by treating x_1 as noise.

$$\gamma_{UE_4}^{x_r,II} = \frac{b_2 P_{UE_3}|g_2|^2}{b_1 P_{UE_3}|g_2|^2 + \sigma^2} = \frac{b_2\eta\epsilon PX_1Y_2}{b_1\eta\epsilon PX_1Y_2 + 1} \tag{15}$$

where $|g_2|^2 \sim Y_2$.

UE_1 decodes x_1 after decoding x_r and cancelling it through SIC.

$$\gamma_{UE_1}^{x_r,II} = \frac{b_2 P_{UE_3}|g_1|^2}{b_1 P_{UE_3}|g_1|^2 + \sigma^2} = \frac{b_2\eta\epsilon PX_1Y_1}{b_1\eta\epsilon PX_1Y_1 + 1} \tag{16}$$

$$\gamma_{UE_1}^{x_1,II} = b_1 P_{UE_3}|g_1|^2 = b_1 P_{UE_3}Y_1 = b_1\eta\epsilon PX_1Y_1 \tag{17}$$

where $|g_1|^2 \sim Y_1$.

B. Decoding Schemes

1) Single Signal Decoding (SDS) Scheme

In the SDS scheme, each of the users, i.e. UE_1, UE_2, UE_3 and U_4 immediately decode the signal after reception. Hence, during the first phase, UE_1, UE_2, and U_3 decode the symbols x_1 and x_2 with the corresponding SINR as shown in Equations (8) - (12). Similarly, during the second phase, UE_1 and UE_4 decode the symbols x_1 and x_r with the corresponding SINR as shown in Equations (15) - (17).

2) Maximal Ratio Combining (MRC) Decoding Scheme

As the achievable data rate is limited by the inferior channel, in the MRC scheme, UE_1 will not immediately decode the received signal in the first phase. UE_1 will instead conserve the signal and jointly decode the signal through the MRC scheme after receiving the decoded symbol x_1 from UE_3 during the second phase. The corresponding SINR during the second stage for the x_1 through the MRC scheme at the UE_1 can be given as:

$$\gamma_{MRC}^{x_1} = \gamma_{UE_1}^{x_1} + \gamma_{UE_1}^{x_1,II} = \frac{a_1 PX_2}{a_2 PX_2 + 1} + b_1\eta\epsilon PX_1Y_1 \tag{18}$$

It should be noted that in our system model, only UE_1 is receiving the data through the direct link and via UE_3. Therefore, MRC is only applied for the signal of UE_1. The users UE_2, UE_3 and UE_4 decode the symbol with the corresponding SINR as explained in the SDS scheme.

III. Ergodic Capacity and Ergodic Sum Capacity

In this section, we explain and derive the analytical expressions for EC for each of the users and the ESC of the entire system for both the SDS and MRC schemes. Since MRC is only applied for the signal of UE_1, the EC of UE_2 and UE_4 remains the same for both SDS and MRC schemes.

A. Ergodic Capacity of UE_1 for SDS

The achievable data rate of UE_1 for the SDS scheme is given by:

$$C_{SDS}^{x_1} = \frac{1}{2}\log_2\left(\left(1+\min(\gamma_{UE_1}^{x_1}, \gamma_{UE_2}^{x_1}, \gamma_{UE_3}^{x_1}, \gamma_{UE_1}^{x_1,II})\right)\right) \tag{19}$$

Theorem 1: The analytical expression for the EC of UE_1 for the SDS scheme can be expressed as:

$$C_{SDS}^{Ana-x_1} = \frac{1}{2\ln 2}\int_{z=0}^{\frac{a_1}{Pa_2}} \frac{P\lambda_{h_1}}{1+zP} e^{-\frac{(\lambda_{h_2}+\lambda_{h_3})z}{(a_1-zPa_2)}} \times \sqrt{\frac{4\lambda_{g_1} z}{b_1\eta\epsilon\lambda_{h_1}}} K_1\left(\sqrt{\frac{4\lambda_{g_1}\lambda_{h_1} z}{b_1\eta\epsilon}}\right) dz \tag{20}$$

where $z = \frac{\gamma}{P}$ and K_1 is modified Bessel function of order 1.
Proof: The proof is given in Appendix A.

B. Ergodic Capacity of UE_1 for the MRC

The achievable data rate of UE_1 for the MRC scheme is given by:

$$C_{MRC}^{x_1} = \frac{1}{2}\log_2\left(\left(1+\min(\gamma_{UE_2}^{x_1}, \gamma_{UE_3}^{x_1}, \gamma_{MRC}^{x_1})\right)\right) \tag{21}$$

Theorem 2: The analytical expression for the EC of UE_1 for the MRC scheme can be expressed as:

$$C_{MRC}^{Ana-x_1} = \frac{1}{2\ln 2}\int_{\gamma=0}^{\infty}\frac{1}{1+\gamma} e^{\frac{\lambda_{h_3}\gamma}{P(a_1-\gamma a_2)}} \int_{x_1=\frac{\gamma}{(1-\epsilon)P(a_1-\gamma a_2)}}^{\infty} \left(\int_{z=c_3}^{\hat{z}} \frac{\lambda_{g_1}}{c_4} e^{\frac{c_2}{c_4}} e^{\frac{\lambda_{g_1}c_3}{c_4}} e^{-\frac{(c_1c_4+c_2c_3)}{c_4 z}} e^{-\frac{\lambda_{g_1} z}{c_4}} dz + e^{-\frac{\lambda_{g_1}\gamma}{b_1\eta\epsilon P x_1}}\right) \lambda_{h_1} e^{-\lambda_{h_1}x_1} dx_1 d\gamma \tag{22}$$

Proof: The proof is given in Appendix B.

C. Ergodic Capacity of UE_2

The achievable data rate of UE_2 is given by:

$$C^{x_2} = \frac{1}{2}\log_2\left(\left(1+\min(\gamma_{UE_2}^{x_2}, \gamma_{UE_3}^{x_2})\right)\right) \tag{23}$$

Theorem 3: The analytical expression for the EC of UE_2 can be expressed as:

$$C_{UE_2}^{Ana-x_2} = \frac{1}{2\ln 2} e^{-\frac{\left(\lambda_{h_1}+\lambda_{h_3}(1-\epsilon)\right)}{a_2(1-\epsilon)P}} E_1\left(e^{-\frac{\left(\lambda_{h_1}+\lambda_{h_3}(1-\epsilon)\right)}{a_2(1-\epsilon)P}}\right) \tag{24}$$

where $E_1(.)$ is exponential integral of order 1.
Proof: The proof can be derived by following the similar steps as in Appendix A and hence it is omitted.

TABLE I. Simulation Parameters

Parameter	Symbol	Values
Mean of $\|h_1\|^2 \rightarrow X_1$	λ_{h_1}	3.5
Mean of $\|h_2\|^2 \rightarrow X_2$	λ_{h_2}	1.5
Mean of $\|h_3\|^2 \rightarrow X_3$	λ_{h_3}	3.0
Mean of $\|g_1\|^2 \rightarrow Y_1$	λ_{g_1}	2.5
Mean of $g_2\|^2 \rightarrow Y_2$	λ_{g_2}	1.5
Source Node Transmit SNR	P	0-45 dB
Energy Harvesting Efficiency	η	0.9
Power Allocation Factor for NOMA	a_1	0.8
Power Allocation Factor for NOMA	a_2	0.2
Power Allocation Factor for NOMA	b_1	0.2
Power Allocation Factor for NOMA	b_2	0.8

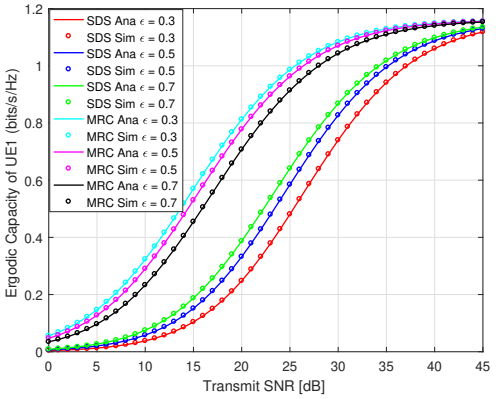

Fig. 2. Ergodic Capacity of UE1

D. Ergodic Capacity of UE_4

The achievable data rate of UE_4 is given by:

$$C_{UE_4}^{x_r} = \frac{1}{2}\log_2\left(\left(1+\min(\gamma_{UE_4}^{x_r,II}, \gamma_{UE_1}^{x_r,II})\right)\right) \tag{25}$$

Theorem 4: The EC of the UE_4 can be expressed as:

$$C_{UE_4}^{Ana-x_r} = \frac{1}{2\ln 2}\times \int_0^{\frac{b_2}{b_1}} \frac{\lambda_{h_1}\sqrt{\frac{4(\lambda_{g_1}+\lambda_{g_2})\gamma}{\eta\epsilon P(b_2-b_1\gamma)\lambda_{h_1}}} K_1\left(\sqrt{\frac{4(\lambda_{g_1}+\lambda_{g_2})\gamma\lambda_{h_1}}{\eta\epsilon P(b_2-b_1\gamma)}}\right)}{1+\gamma} d\gamma \tag{26}$$

Proof: The proof is straightforward and can be derived by following the similar steps as in Appendix A.

E. Ergodic Sum Capacity

Now, combining Equations (20), (24) and (26) gives the analytical expression for the ESC of the system for the SDS scheme. Similarly, combining Equations (21), (24) and (26) gives the analytical expression for the ESC of the system for the MRC scheme.

It should be noted that the integral terms in Equations (20), (22), (24) and (26) are difficult to evaluate in closed form. However, it can be solved through numerical approaches using softwares such as Matlab or Mathematica.

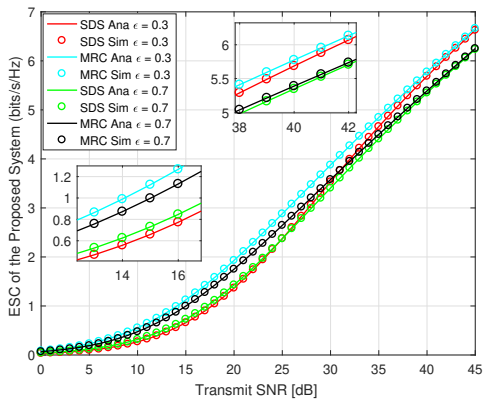

Fig. 3. ESC of the Proposed System

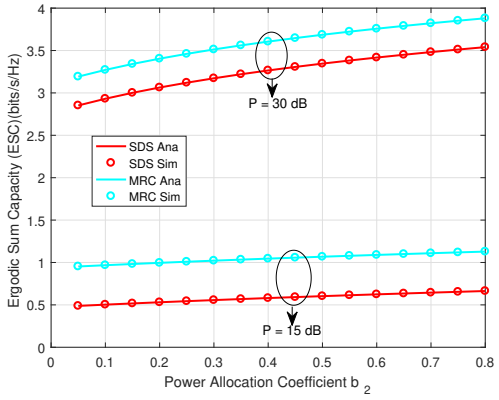

Fig. 4. ESC of the Proposed System vs Power Allocation Coefficient b_2

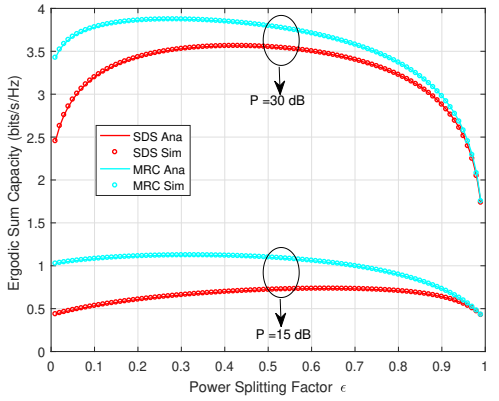

Fig. 5. ESC of the Proposed System vs Power Splitting Factor

IV. Numerical Results

In this section, we verify our derived mathematical analysis for the EC and ESC with Monte-Carlo simulation results. The simulation parameters used for the experiments are as listed in Table I, unless otherwise stated. We have used MATLAB for running the Monte-Carlo experiments by averaging over 10^5 random realization of Rayleigh fading channels i.e., h_1, h_2, h_3, g_1 and g_2.

In Fig. 2, we plot the EC of UE_1 against the transmit SNR. Since, in our considered system model, the UE_1 node is receiving its data through a direct link from the BS and via an EH based relay UE_3, we observe that the MRC scheme outperforms the SDS scheme against all transmit SNR values. This indicates the performance gain in the EC of UE_1 node by consolidating direct link and using the MRC scheme compared to the SDS scheme. For both the SDS and MRC schemes, the EC is an increasing function with respect to increase in transmit SNR. Also, it is interesting to note that as we increase the power splitting factor from $\epsilon = 0.3$ to $\epsilon = 0.7$, the EC increases for the SDS scheme. However, the EC decreases for the MRC scheme as we increase the ϵ from 0.3 to 0.7. This indicates that lower ϵ is sufficient for the MRC scheme while higher ϵ is required for the SDS scheme to harvest more energy for the data transmission. Higher ϵ implies that UE_3 can harvest more energy and it can transmit the signal of UE_1 with more power.

Taking UE_1, UE_2, and UE_4 as three users in the considered system, we plot the ESC of the system against the transmit SNR at ϵ = 0.3 and 0.7 in Fig. 3. As expected, we see that the MRC scheme outperforms the SDS scheme. However, the ESC difference between MRC and SDS is clearly seen when the transmit SNR is less than 35 dB. When the transmit SNR is above 35 dB, the ESC difference between the MRC and SDS schemes becomes very small and eventually negligible. The reason for this is that at such high transmit SNR, i.e., above 35 dB, the relay node UE_3 can harvest more energy, which eventually increases the ESC of the SDS scheme. It should be noted that in our considered system, the MRC scheme is only applied to the UE_1 user since it receives data through the direct link and via UE_3.

In Fig. 4, we plot the ESC against the power allocation coefficient factor b_2 at $\epsilon = 0.3$ and at transmit SNR 15 dB and 30 dB. The reason for choosing b_2 for this plot is that b_2 is assigned to the distant D2D user UE_4, which determines the fraction of harvested energy utilized by UE_3 for transmitting the data to UE_4. For this plot, the other power allocation coefficient factor b_1 is fixed at 0.2. We see that at transmit SNR 30 dB, the ESC for both the MRC and SDS schemes increases with an increase in b_2. However, at transmit SNR 15 dB, the ESC curve looks almost saturated when the b_2 factor is 0.3 and above for both the MRC and SDS schemes. This indicates that the b_2 factor plays a dominant role in increasing the ESC of the system, especially at high transmit SNR. For a NOMA-SWIPT system, it is obvious that the relay UE_3 can harvest more energy at higher transmit SNR, which will eventually increase the ESCs of the SDS and MRC schemes with a proper selection of the power allocation coefficient factor b_2.

In Fig. 5, we plot the ESC of the system against the power splitting factor ϵ at transmit 15 dB, and 30 dB. We observe that the ESC for the SDS and MRC schemes first increases with an increase in ϵ until it reaches a maximum point, and then it starts decreasing. This suggests that that the ESC is a concave

function and it has a maxima at which the ESC of both SDS and MRC schemes is maximized. In principle, we cannot have a too high ϵ value, since then too much power will be allocated for EH and too little power for information decoding at the UE_3. Therefore, finding an optimal ϵ is important for the ESC maximization of the considered system. The optimal ϵ can be found out by the Golden section search method as in [21].

V. Conclusions and Future Work

In this paper, we investigated the EC and ESC performance of a NOMA-SWIPT aided D2D IoT relay system with direct links. A two-user case was studied where a BS transmitted two symbols to two users through the direct link and via an EH based relay node in the first stage. The EH based relay node harvested the energy from the signal of the BS using the PS architecture and re-transmitted the data of the distant user with poor channel conditions from the first stage and the data for its D2D user using a NOMA protocol in the second stage. Analytical expression for the ECs of each of the user node and the overall ESC of the system using MRC and SDS schemes were mathematically derived and verified with the Monte-Carlo simulation results. Effect of transmit SNR and EH parameter-power splitting factor and power allocation coefficient factor for NOMA on the EC and ESC performance for both the MRC and SDS schemes were studied and investigated. Our results demonstrated that the EC of a node and the ESC of the NOMA-SWIPT aided D2D IoT relay system with direct link can be improved through the MRC scheme compared to the SDS scheme. Finally, our results also demonstrated that, by having a direct link and using the MRC scheme for a single user, the ESC of the whole system can be improved.

For the future work, we would like to investigate the outage probability and do a thorough comparison of the considered system model with other energy harvesting architectures. Also, studying the effect of interference and secrecy capacity in the presence of eavesdroppers is an interesting topic for our future work.

Appendix A
Proof of Theorem 1

The cumulative distributive function (CDF) of $\min(\gamma_{UE_1}^{x_1}, \gamma_{UE_2}^{x_1}, \gamma_{UE_3}^{x_1}, \gamma_{UE_1}^{x_1,II})$ can be expressed as:

$$F_\gamma(\gamma) = 1 - \Pr\left(X_2 \geq \frac{\gamma}{P(a_1-\gamma a_2)}\right)\Pr\left(X_3 \geq \frac{\gamma}{P(a_1-\gamma a_2)}\right)\Pr\left(X_1 \geq \frac{\gamma}{(1-\epsilon)P(a_1-\gamma a_2)}, Y_1 \geq \frac{\gamma}{b_1\eta\epsilon P X_1}\right)$$

Now, conditioning X_1, we get,

$$F_\gamma(\gamma) = 1 - e^{-\frac{\gamma\lambda_{h_2}}{P(a_1-\gamma a_2)}} e^{-\frac{\gamma\lambda_{h_3}}{P(a_1-\gamma a_2)}} \int_{x_1=0}^{\infty} \Pr\left(x_1 \geq \frac{\gamma}{(1-\epsilon)P(a_1-\gamma a_2)}, Y_1 \geq \frac{\gamma}{b_1\eta\epsilon P x_1}\right) f_{X_1}(x_1)dx_1$$

$$F_\gamma(\gamma) = 1 - e^{-\frac{(\lambda_{h_2}+\lambda_{h_3})\gamma}{P(a_1-\gamma a_2)}} \times \int_{x_1=\frac{\gamma}{(1-\epsilon)P(a_1-\gamma a_2)}}^{\infty} \Pr\left(Y_1 \geq \frac{\gamma}{b_1\eta\epsilon P x_1}\right) f_{X_1}(x_1)dx_1$$

$$F_\gamma(\gamma) = 1 - e^{-\frac{(\lambda_{h_2}+\lambda_{h_3})\gamma}{P(a_1-\gamma a_2)}} \times \int_{x_1=\frac{\gamma}{(1-\epsilon)P(a_1-\gamma a_2)}}^{\infty} \lambda_{h_1} e^{-\frac{\lambda_{g_1}\gamma}{b_1\eta\epsilon P x_1} - \lambda_{h_1}x_1} dx_1$$

Now,

The EC in terms of the CDF $F_\gamma(\gamma)$ can be written as:

$$C_{SDS}^{Ana-x_1} = \frac{1}{2\ln 2}\int_{\gamma=0}^{\infty} \frac{1}{1+\gamma}[1-F_\gamma(\gamma)]d\gamma$$

$$C_{SDS}^{Ana-x_1} = \frac{1}{2\ln 2}\int_{\gamma=0}^{\infty} \frac{\lambda_{h_1}}{1+\gamma} e^{-\frac{(\lambda_{h_2}+\lambda_{h_3})\gamma}{P(a_1-\gamma a_2)}} \times \int_{x_1=\frac{\gamma}{(1-\epsilon)P(a_1-\gamma a_2)}}^{\infty} e^{-\frac{\lambda_{g_1}\gamma}{b_1\eta\epsilon P x_1} - \lambda_{h_1}x_1} dx_1 d\gamma$$

Let $z = \frac{\gamma}{P} \rightarrow \gamma = zP \rightarrow d\gamma = Pdz$

$$C_{SDS}^{Ana-x_1} = \frac{1}{2\ln 2}\int_{z=0}^{\infty} \frac{P\lambda_{h_1}}{1+zP} e^{-\frac{(\lambda_{h_2}+\lambda_{h_3})z}{(a_1-zPa_2)}} \times \int_{x_1=0}^{\infty} \lambda_{h_1} e^{-\frac{-\lambda_{g_1}z}{b_1\eta\epsilon x_1} - \lambda_{h_1}x_1} dx_1 dz$$

$$C_{SDS}^{Ana-x_1} = \frac{1}{2\ln 2}\int_{z=0}^{\frac{a_1}{Pa_2}} \frac{P\lambda_{h_1}}{1+zP} e^{-\frac{(\lambda_{h_2}+\lambda_{h_3})z}{(a_1-zPa_2)}} \times \int_{x_1=0}^{\infty} e^{-\frac{-\lambda_{g_1}z}{b_1\eta\epsilon x_1} - \lambda_{h_1}x_1} dx_1 dz$$

$$C_{SDS}^{Ana-x_1} = \frac{1}{2\ln 2}\int_{z=0}^{\frac{a_1}{Pa_2}} \frac{P\lambda_{h_1}}{1+zP} e^{-\frac{(\lambda_{h_2}+\lambda_{h_3})z}{(a_1-zPa_2)}} \times \sqrt{\frac{4\lambda_{g_1}z}{b_1\eta\epsilon\lambda_{h_1}}} K_1\left(\sqrt{\frac{4\lambda_{g_1}\lambda_{h_1}z}{b_1\eta\epsilon}}\right) dz$$

This completes the proof of Theorem 1.

Appendix B
Proof of Theorem 2

The CDF of $\min(\gamma_{UE_2}^{x_1}, \gamma_{UE_3}^{x_1}, \gamma_{MRC}^{x_1})$ can be expressed as:

$$F_\gamma(\gamma) = 1 - \Pr\left(\frac{a_1PX_3}{a_2PX_3+1} \geq \gamma\right)\Pr\left(\frac{a_1(1-\epsilon)PX_1}{a_2(1-\epsilon)PX_1+1} \geq \gamma, \frac{a_1PX_2}{a_2PX_2+1} + b_1\eta\epsilon PX_1Y_1 \geq \gamma\right)$$

$$F_\gamma(\gamma) = 1 - \Pr\left(X_3 \geq \frac{\gamma}{P(a_1-\gamma a_2)}\right)\Pr\left(X_1 \geq \frac{\gamma}{(1-\epsilon)P(a_1-\gamma a_2)}, \frac{a_1PX_2}{a_2PX_2+1} \geq \gamma - b_1\eta\epsilon PX_1Y_1\right)$$

Conditioning on X_1, we get,

$$F_\gamma(\gamma) = 1 - e^{\frac{\lambda_{h_3}\gamma}{P(a_1-\gamma a_2)}} \int_{x_1=\frac{\gamma}{(1-\epsilon)P(a_1-\gamma a_2)}}^{\infty} \Pr\left(\frac{a_1PX_2}{a_2PX_2+1} \geq \gamma - b_1\eta\epsilon Px_1Y_1\right) f_{X_1}(x_1)dx_1$$

Conditioning on Y_1, we get,

$$F_\gamma(\gamma) = 1 - e^{\frac{\lambda_{h_3}\gamma}{P(a_1-\gamma a_2)}} \int_{x_1=\frac{\gamma}{(1-\epsilon)P(a_1-\gamma a_2)}}^{\infty} \underbrace{\int_{y_1=0}^{\infty}}$$

$$\underbrace{\Pr\left(\frac{a_1 P X_2}{a_2 P X_2 + 1} \geq \gamma - b_1\eta\epsilon P x_1 y_1\right) f_{Y_1}(y_1) dy_1}_{I_1} f_{X_1}(x_1) dx_1$$

Now, $\gamma = b_1\eta\epsilon P x_1 y_1 \rightarrow y_1 = \dfrac{\gamma}{b_1\eta\epsilon P x_1}$

$$I_1 = \underbrace{\int_{y_1=0}^{\frac{\gamma}{b_1\eta\epsilon P x_1}} \Pr\left(\frac{a_1 P X_2}{a_2 P X_2 + 1} \geq \gamma - b_1\eta\epsilon P x_1 y_1\right) f_{Y_1}(y_1) dy_1}_{J_1}$$

$$+ \underbrace{\int_{y_1=\frac{\gamma}{b_1\eta\epsilon P x_1}}^{\infty} f_{Y_1}(y_1) dy_1}_{J_2}$$

$$J_1 = \int_{y_1=0}^{\frac{\gamma}{b_1\eta\epsilon P x_1}} \Pr\left(X_2 \geq \frac{\gamma - b_1\eta\epsilon P x_1 y_1}{a_1 P - a_2 P\gamma + a_2 P b_1\eta\epsilon P x_1 y_1}\right)$$

$$\lambda_{g_1} e^{-\lambda_{g_1} y_1} dy_1$$

$$J_1 = \int_{y_1=0}^{\frac{\gamma}{b_1\eta\epsilon P x_1}} e^{\frac{-\lambda_{h_2}\gamma + b_1\eta\epsilon P\lambda_{h_2} x_1 y_1}{a_1 p - a_2 P\gamma + a_2 P b_1\eta\epsilon P x_1 y_1}} \lambda_{g_1} e^{-\lambda_{g_1} y_1} dy_1$$

Let, $c_1 = \lambda_{h_2}\gamma, c_2 = b_1\eta\epsilon P\lambda_{h_2} x_1, c_3 = a_1 P - a_2 P\gamma$

$c_4 = a_2 P b_1\eta\epsilon P x_1$

$$J_1 = \int_{y_1=0}^{\frac{\gamma}{b_1\eta\epsilon P x_1}} \lambda_{g_1} e^{\frac{-c_1 + c_2 y_1}{c_3 + c_4 y_1} - \lambda_{g_1} y_1} dy_1$$

Now, put $c_3 + c_4 y_1 = z \rightarrow dy_1 = \dfrac{1}{c_4} dz$

Also, when $y_1 = 0, z = c_3$ and, when

$y_1 = \dfrac{\gamma}{b_1\eta\epsilon P x_1}, z = c_3 + c_4 \dfrac{\gamma}{b_1\eta\epsilon P x_1} \rightarrow \hat{z}$

$$J_1 = \int_{z=c_3}^{\hat{z}} \frac{\lambda_{g_1}}{c_4} e^{\frac{-c_1 + c_2\frac{z-c_3}{c_4}}{z} - \lambda_{g_1}\left(\frac{z-c_3}{c_4}\right)} dz$$

$$J_1 = \int_{z=c_3}^{\hat{z}} \frac{\lambda_{g_1}}{c_4} e^{\frac{c_2}{c_4}} e^{\frac{\lambda_{g_1} c_3}{c_4}} e^{-\frac{(c_1 c_4 + c_2 c_3)}{c_4 z} - \frac{\lambda_{g_1} z}{c_4}} dz$$

Now,$J_2 = \displaystyle\int_{y_1=\frac{\gamma}{b_1\eta\epsilon P x_1}}^{\infty} \lambda_{g_1} e^{-\lambda_{g_1} y_1} dy_1 = e^{-\frac{\lambda_{g_1}\gamma}{b_1\eta\epsilon P x_1}}$

Now,$I_1 = J_1 + J_2$

$$I_1 = \int_{z=c_3}^{\hat{z}} \frac{\lambda_{g_1}}{c_4} e^{\frac{c_2}{c_4}} e^{\frac{\lambda_{g_1} c_3}{c_4}} e^{-\frac{(c_1 c_4 + c_2 c_3)}{c_4 z} - \frac{\lambda_{g_1} z}{c_4}} dz + e^{-\frac{\lambda_{g_1}\gamma}{b_1\eta\epsilon P x_1}}$$

Now,

$$F_\gamma(\gamma) = 1 - e^{\frac{\lambda_{h_3}\gamma}{P(a_1 - \gamma a_2)}} \int_{x_1=\frac{\gamma}{(1-\epsilon)P(a_1-\gamma a_2)}}^{\infty} \left(\int_{z=c_3}^{\hat{z}} \frac{\lambda_{g_1}}{c_4} e^{\frac{c_2}{c_4}} e^{\frac{\lambda_{g_1} c_3}{c_4}} e^{-\frac{(c_1 c_4 + c_2 c_3)}{c_4 z} - \frac{\lambda_{g_1} z}{c_4}} dz + e^{-\frac{\lambda_{g_1}\gamma}{b_1\eta\epsilon P x_1}} \right) \lambda_{h_1} e^{-\lambda_{h_1} x_1} dx_1$$

Now, the EC in terms of the CDF $F_\gamma(\gamma)$ can be written as:

$$C_{MRC}^{Ana-x_1} = \frac{1}{2\ln 2} \int_{\gamma=0}^{\infty} \frac{1}{1+\gamma} [1 - F_\gamma(\gamma)] d\gamma$$

Substituting $F_\gamma(\gamma)$ in the above equation, we get the final expression as in Equation (22).

This ends the proof of Theorem 2.

REFERENCES

[1] J. Jin, J. Gubbi, S. Marusic, and M. Palaniswami, "An information framework for creating a smart city through internet of things," *IEEE Internet of Things journal*, vol. 1, no. 2, pp. 112–121, 2014.

[2] J. Howell, "Number of connected iot devices will surge to 125 billion by 2030," *IHS markit says*, 2017, https://sst.semiconductor-digest.com/2017/10/number-of-connected-iot-devices-will-surge-to-125-billion-by-2030/.

[3] S. Li, L. Da Xu, and S. Zhao, "5g internet of things: A survey," *Journal of Industrial Information Integration*, vol. 10, pp. 1–9, 2018.

[4] P. Gandotra, R. K. Jha, and S. Jain, "Green communication in next generation cellular networks: A survey," *IEEE Access*, vol. 5, pp. 11 727–11 758, 2017.

[5] N. Shafiee, S. Tewari, B. Calhoun, and A. Shrivastava, "Infrastructure circuits for lifetime improvement of ultra-low power iot devices," *IEEE Transactions on Circuits and Systems I: Regular Papers*, vol. 64, no. 9, pp. 2598–2610, 2017.

[6] A. Orsino, G. Araniti, L. Militano, J. Alonso-Zarate, A. Molinaro, and A. Iera, "Energy efficient iot data collection in smart cities exploiting d2d communications," *Sensors*, vol. 16, no. 6, p. 836, 2016.

[7] Y. Xu, C. Shen, Z. Ding, X. Sun, S. Yan, G. Zhu, and Z. Zhong, "Joint beamforming and power-splitting control in downlink cooperative swipt noma systems," *IEEE Transactions on Signal Processing*, vol. 65, no. 18, pp. 4874–4886, 2017.

[8] K. Higuchi and A. Benjebbour, "Non-orthogonal multiple access (noma) with successive interference cancellation for future radio access," *IEICE Transactions on Communications*, vol. 98, no. 3, pp. 403–414, 2015.

[9] Z. Ding, X. Lei, G. K. Karagiannidis, R. Schober, J. Yuan, and V. K. Bhargava, "A survey on non-orthogonal multiple access for 5g networks: Research challenges and future trends," *IEEE Journal on Selected Areas in Communications*, vol. 35, no. 10, pp. 2181–2195, 2017.

[10] J. Li, W. Liu, T. Wang, H. Song, X. Li, F. Liu, and A. Liu, "Battery-friendly relay selection scheme for prolonging the lifetimes of sensor nodes in the internet of things," *IEEE Access*, vol. 7, pp. 33 180–33 201, 2019.

[11] L. R. Varshney, "Transporting information and energy simultaneously," in *2008 IEEE International Symposium on Information Theory*. IEEE, 2008, pp. 1612–1616.

[12] T. D. P. Perera and D. N. K. Jayakody, "Analysis of time-switching and power-splitting protocols in wireless-powered cooperative communication system," *Physical Communication*, vol. 31, pp. 141–151, 2018.

[13] H. Q. Tran, C. V. Phan, and Q.-T. Vien, "Power splitting versus time switching based cooperative relaying protocols for swipt in noma systems," *Physical Communication*, p. 101098, 2020.

[14] A. Rauniyar, P. Engelstad, and O. N. Østerb, "Rf energy harvesting and information transmission based on power splitting and noma for iot relay systems," in *2018 IEEE 17th International Symposium on Network Computing and Applications (NCA)*. IEEE, 2018, pp. 1–8.

[15] A. Rauniyar, P. E. Engelstad, and O. N. Østerbø, "Performance analysis of rf energy harvesting and information transmission based on noma with interfering signal for iot relay systems," *IEEE Sensors Journal*, vol. 19, no. 17, pp. 7668–7682, Sep. 2019.

[16] J.-B. Kim, I.-H. Lee, and J. Lee, "Capacity scaling for d2d aided cooperative relaying systems using noma," *IEEE Wireless Communications Letters*, vol. 7, no. 1, pp. 42–45, 2017.

[17] C. Liu and T. Lv, "Joint relay-user selection in energy harvesting relay network with direct link," *Physical Communication*, vol. 28, pp. 123–129, 2018.

[18] Y. Ye, Y. Li, F. Zhou, N. Al-Dhahir, and H. Zhang, "Power splitting-based swipt with dual-hop df relaying in the presence of a direct link," *IEEE Systems Journal*, vol. 13, no. 2, pp. 1316–1319, 2018.

[19] D.-B. Ha and S. Q. Nguyen, "Outage performance of energy harvesting df relaying noma networks," *Mobile Networks and Applications*, vol. 23, no. 6, pp. 1572–1585, 2018.

[20] M. B. Uddin, M. F. Kader, and S. Y. Shin, "Uplink cooperative diversity using power-domain nonorthogonal multiple access," *Transactions on Emerging Telecommunications Technologies*, p. e3678, 2019.

[21] A. Rauniyar, P. Engelstad, and O. Østerbø, "Rf energy harvesting and information transmission based on noma for wireless powered iot relay systems," *Sensors*, vol. 18, no. 10, p. 3254, 2018.